



ORIGINAL ARTICLE

Optimization of Cadmium Removal from Aqueous Solutions Using Walnut-shell Residues Biochar Supported/unsupported by Nanoscale Zero-valent Iron through Response Surface Methodology

Mahboub Saffari

Environment Department, Institute of Science and High Technology and Environmental Sciences, Graduate University of Advanced Technology, Kerman, Iran

(Received: 30 October 2017 Accepted: 31 January 2018)

KEYWORDS

Box Behnken design;
Biochar;
Heavy metal;
Nanocomposite

ABSTRACT: Using various biochars to remove heavy metals (HMs) from aqueous solutions has been increased in recent years. It is believed that the use of nanocompounds in biochars surface structure may increase the efficiency of contaminants removal. Therefore, this research tries to investigate the efficiency of walnut-shell biochar (WSB) alone or supported by nanoscale zero-valent iron (WSB-nZVI) on cadmium (Cd) removal in aqueous solution controlled by four variables including initial Cd concentration, initial solution pH, contact time, and adsorbent dosage by Box Behnken design under response surface methodology. The results of present study showed that WSB-nZVI has a significant priority on WSB of Cd removal efficiency in aqueous solutions. The existence of functional groups on the surface of WSB via precipitation and adsorption processes, as well as nZVI formed on the WSB-nZVI via generating adsorption and complexation processes, have increased the ability Cd removal than WSB raw adsorbent. The maximum predicted Cd removal efficiency based on the proposed model was 99.72% with desirability of 1, in initial Cd concentration of 70.78 mg L⁻¹, pH of 6.92, adsorbent dose of 0.56 g L⁻¹ and contact time of 40.42 min.

INTRODUCTION

The environment pollution by various pollutants, including HMs, has become a global challenge and problem due to urbanization spreading and human industrial activities [1].

High amounts of HMs in water sources effects diversely on human health and leads to non-consumable water [2].

Metals could enter into water sources naturally or through human. Natural weathering of rocks and soils that are in contact with water sources, are the largest natural source of water pollution to HMs [3]. Mining, the disposal of unrefined or semi-refined wastewaters containing HMs, and the use of fertilizers containing HMs

*Corresponding Author: mahboobsaffari@gmail.com (M. Saffari)

(such as phosphate fertilizers) are the main sources of HMs pollution. HMs can accumulate in the beings' body and cause various diseases, disabilities, and cancer, due to their indissoluble nature and high toxicity [4]. Among HMs, Cd is one of these elements with utmost toxicity to human. Cd doses of 10 to 326 and 300 to 3500 mg are toxic and deadly to humans, respectively, and their continuous and prolonged contact causes disruption of renal function [5].

In order to remove HMs from aqueous solution, some common methods including chemical precipitation, ion exchange, extraction by plants, ultrafiltration, reverse osmosis, electro-dialysis and sorption had been used [6]. The sorption process has been used as an effective and economical way to remove HMs in recent decades [7]. Agricultural wastes are introduced as one of the most important wastes among five wastes classified as waste management. The high cost of waste management has brought a heavy burden on the economy of the country; therefore, it is very important to pay attention to agricultural wastes management to achieve sustainable development. Commercial activated carbon (CAC) is one of the most common adsorbent materials for removing various pollutants, but applying CAC is much cost to do so. Today, the researchers are seeking to obtain low-cost adsorbent materials instead of CAC, so that the study on HMs removal from water and wastewater by low cost adsorbents from agricultural waste products [8] such as biochar, has been considerable. Biochar is a coal-like material obtained from plant biomasses and agricultural wastes, which produced during the pyrolysis processes [9]. It is composed of carbon, with a high porosity, high special surface area, and high ability to adsorb various pollutants including HMs [10].

Recently, some researchers believe that the application of raw biochar in highly contaminated water solution cannot act effectively on the pollutants removal [11]; therefore, in order to solve this problem, they proposed engineered biochars with new structures and different

surface properties [12, 13]. In recent years, the application of nano-composite-based biochars has been considered as one of the engineered biochars to remove pollutants of aquatic environments [12, 14]. Waste management, pollutants removal, carbon sequestration, and energy production are four integrated goals, obtained from synthesis of nano-materials-based biochars [15].

Nanoscale zero valent iron (nZVI) has been used in many experiments as an effective adsorbent to remove HMs such as Cd^{2+} [16], As^{5+} [17], Cr^{6+} [18], and Pb^{2+} [19], due to have reducing processes, formation of adsorption, and precipitation complexes. The nZVI particles agglomeration makes some limitation in the migration of these materials throughout the solution, and as a result, it reduces the efficiency of this adsorbent [20]. Therefore, it seems that the presence of nZVI as a support material on a solid surface may increase their stability in aqueous environments.

Recognizing the major factors affecting the removal of HMs from aqueous solutions can help researchers to achieve their optimal goals. Achieving this optimal level requires a lot of experiments and expenses, so in order to solve this problem, response surface methodology (RSM) is introduced as an alternative method with minimum testing. This method tries to find a certain relation between one or more dependent responses and a certain number of non-dependent variables by using mathematical systems [21].

According to mentioned introduction, and since many studies have focused solely on the efficacy of various biochars supported by nZVI on organic pollutants, so this research tries to investigate the efficiency of walnut-shell biochar (WSB) alone or supported by nanoscale zero-valent iron (WSB-nZVI) on Cd removal in aqueous solution under different condition of experiments including Cd concentration, solution pH, contact time, and dosage of adsorbents, using Box–Behnken design (BBD), under RSM.

MATERIALS AND METHODS

Chemicals

Chemical used in this study, except cadmium nitrate, including iron sulfate heptahydrate ($\text{FeO}_4\text{S}\cdot 7\text{H}_2\text{O}$), sodium borohydride (NaBH_4), hydrochloric acid fuming 37% (HCl), sodium hydroxide (NaOH) were purchased from Merck. Cadmium nitrate ($\text{Cd}(\text{NO}_3)_2\cdot 4\text{H}_2\text{O}$) was purchased from Scharlau products Co. All solutions were prepared using distilled water.

Preparation and characterization of adsorbents

The walnut-shell residues (WS) were used as raw feedstocks to produce biochar. For this purpose, firstly, the WS were washed with distilled water several times and dried in an air-forced oven at 60°C for 48 h. Then, the samples were chopped and passed through a 4 mm sieve. Raw feedstocks were pyrolysed in a muffle furnace, under a limited oxygen condition, for 4h at 500°C to produce walnut-shell biochar (WSB). To provide oxygen-limiting conditions, pure nitrogen gas was injected into the muffle furnace at a flow rate of 5 liters per minute for 5 minutes. Biochar electrical conductivity (EC) and pH were measured using 1:5 solid: water ratio after shaking for 30 min [22]. Elemental C, N, H, and S abundances were determined, using a CHNS Elemental Analyzer (varioMACRO CHNS). The WSB supported by nanoscale zero-valent iron (WSB-nZVI) was produced according to producers reported by Quan et al. [23]. According to this method, initially, the pretreatment process will be performed on biochar samples. For this purpose, 10.0 g of the WSB was added to 250 ml of sulfuric acid (0.05 M) at 45°C for 48 h under mechanical string at 300 rpm, then washed with distilled water and dried. In next stage, based on a conventional liquid-phase method, 2 g of pretreated biochar was suspended in 60-mL 1.0 M FeSO_4 and stirred for 2 h to adsorb Fe^{2+} onto biochar. Then, 90-mL ethanol (50%) was added, and 100-mL 0.4 M of sodium borohydride was added

drop by drop (1 drop per 2s) to the suspension and kept continuous stirring for 2 h to complete the reaction. In order to prevent oxidation, all of the above steps will be carried out in the presence of nitrogen gas. At the end, the suspension was centrifuged and washed three times with pure ethanol (96%) to avoid the immediate oxidation of WSB-nZVI [23], and put in a vacuum drying oven at 60°C for 8 h. Finally, the prepared WSB-nZVI was stored inside the glove box before using. The structure of WSB and WSB-nZVI were examined with an X-ray diffraction (Bruker D8 Advance X-ray diffractometer with Cu $K\alpha$ radiation operated at 40 kV and 40 mA), Fourier transform infrared spectroscopy (FTIR; TENSOR II from Bruker), and field emission scanning electron microscope (Fe-SEM; TESCAN FE-SEM MIRA3).

Batch experiments

A series of batch experiments were conducted to determine the effects of independent variables, including initial Cd concentration, solution pH, kinds of adsorbent, contact time, and dosage of adsorbents, on Cd removal from Cd aqueous solutions. For this purpose, 25 ml solution containing different levels of Cd (25, 50, and 75 mg L^{-1}) with the desired pH (3, 5, and 7; set by 0.1 M NaOH and 0.1 M HCl solutions) were poured into centrifuge tubes, and prepared adsorbents (WSB and WSB-nZVI) at different dosages (0.5 , 1.5 and 2 g L^{-1}) were added to each tube separately. Tubes were shaken vigorously for 20, 40, and 60 min at 25°C , and then centrifuged at 3000 rpm. The supernatant was filtered, and the concentration of Cd in the clear extract solution was determined using atomic absorption spectrophotometer (Varian Spectr AA-10). The percentage of Cd removal (R) was calculated from Equation,

$$R = \frac{C_i - C_f}{C_i} \times 100$$

where C_i and C_f are initial and final Cd concentrations (mg L^{-1}), respectively.

Experimental design and optimization of adsorption process using RSM approach

In present study, Box–Behnken model (BBM) under RSM was used as experimental design model to determine the optimum condition of Cd removal from aqueous solutions. The RSM has been introduced as an operative model which contains of a group of dedicated empirical techniques to prediction of relationship between a group of controlled investigational factors and measured responses according to one or more selected criteria. BBM are rotatable or nearly rotatable second-order designs based on three-level incomplete factorial designs [24]. For three factors BBM, its graphical representation can be seen as a cube that consists of the central point and the middle points of the edges [25, 26]. Optimization experiments were carried out by evaluation the effect of four variables including Cd concentration, solution pH, contact time, and dosage of adsorbents; at three levels: high, medium and low, and 1 category contained 2 variables (WSB and WSB-nZVI). Codification of the levels of the independent variables, which is converting real value into coordinates inside a scale with dimensionless values, were done according to the following equation:

x_i : dimensionless value of an independent variable

X_i : real value of an independent variable

X_0 : value of an independent variable at the center point

ΔX_i : step change

The number of experiments required by BBM was determined from the relation $N=2K(K-1)+C$, where N is the number of test samples, K is the number of variables (4 variables), and C is the number of central points (5 central points). In this study, the total of experiments based on BBD was 58 tests (29 tests for WSB and 29 tests for WSB-nZVI). An empirical second-order polynomial model is used to determine the relationship be-

tween removal efficiency of Cd (as the dependent variable) and behavior of the system (as the independent variables), which is expressed:

$$Y = \alpha + \sum \beta_i X_i + \sum \beta_{ii} X_i^2 + \sum \beta_{ij} X_i X_j + \varepsilon$$

where Y is the response, α , β_i , β_{ii} are the regression coefficients of variables for intercept, linear, quadratic and interaction terms, respectively. X_i and X_j are the independent variables and ε is the residual term. Regression equations and response surface plots of RSM, for identification of optimum conditions of Cd removal, were generated by design-expert software (version 7.00).

$$x_i = \frac{X_i - X_0}{\Delta X_i}$$

RESULTS AND DISCUSSION

Characteristics of the produced adsorbent materials

The elemental analysis of WS, WSB, and WSB-nZVI, containing percentage of hydrogen (H), carbon (C), nitrogen (N), and sulfur (S), has been presented in Table 1. Applying the pyrolysis process on WS has increased C and reduced H, N and S. Increasing and decreasing C and H in the WSB sample, respectively, may be attributed to carbonation processes and the loss of H-containing functional groups. European Biochar Certificate (EBC, 2012) refers to a substance called biochar, containing at least 50% C, in which H/C maximum ratio is about 0.7. According to the obtained results, the produced biochar had 53.6% C and the H/C ratio was 0.04, which confirms the proper production of biochar in the present study. The amounts obtained from pH and EC of produced biochar showed that pyrolysis process increased pH (from 7.1 to 8.3) as well as EC (0.1 to 2.3 dS m^{-1}) as a result of increasing the base functional groups and base cations in the weight unit of produced biochar [27]. In order to investigate the effect of adding nZVI to biochar, the elemental analysis of this substance showed

a decrease in pH as compared to WSB, which can be attributed to several times washing of WSB by acid and distilled water and, consequently the release of soluble base cations before the production of WSB-nZVI. Also, the results obtained from the elemental analysis of WSB-nZVI showed higher levels of H and less level of C and N compared to WSB. The increase of H content in the WSB-nZVI sample may be justified by the production of H gas during the nZVI precipitation process on the WSB. FTIR spectroscopy was performed to determine the quality of the functional groups of produced adsorbent substances compared to WS (Figure 1). The results show a lot of variations in the spectra created in all three samples studied. The pyrolysis process has reduced the intensity of the two band spectra peaks of 3373 cm^{-1} ($3200\text{ to }3500\text{ cm}^{-1}$) and 2923 cm^{-1} ($2820\text{ to }2980\text{ cm}^{-1}$), indicating the presence of hydroxyl and aliphatic functional groups, respectively. Sharma et al. [28] also found similar results, and indicated the reason as demethoxylation, dehydration, and demethylation of lignin. According to the results, the pyrolysis process has led to the disappearance of the 1611 cm^{-1} band, indicating the presence of the C-N group, which can be explained by the sublimation of nitrogen forms in produced biochar. The presence and absence of the 1574 cm^{-1} peak in WSB and WS, respectively, indicate the presence of C=O aromatic groups in WSB. The resulting band in 1061 cm^{-1} in the WS sample, which shows the C-O groups of carbohydrates, was disappeared as a result of pyrolysis process. The comparison of the functional groups in WSB and WS showed that the pyrolysis process increased some functional groups

such as C=O aromatic and carboxylic bands (including -COOH). The FTIR spectroscopy of the WSB-nZVI sample was also performed to investigate the changes caused by the formation of a layer of nZVI on biochar. The results of the WSB-nZVI spectroscopy showed that the spectra bands of 1574 , 1393 , and 1318 cm^{-1} have been disappeared due to nZVI coating on biochar, which could be attributed to the interaction effects of $\text{Fe}^{3+}/\text{Fe}^0$ on the biochar functional groups surface [29]. Also, the WSB-nZVI FTIR results have indicated the disappearance of the 2913 cm^{-1} spectrum in WS and WSB, which can be explained by the elimination of polar functional groups during the nZVI precipitation process on biochar [29]. The existence of the 460 cm^{-1} spectrum, which is related to the presence of Fe-O, in the WSB-nZVI sample, differs significantly from the other two samples. In general, according to the FTIR analysis results, it can be stated that the pyrolysis process has increased the biochar aromatic properties. Also, the presence of nZVI causes changes in the biochar functional groups, which, in some cases, have eliminated some biochar functional groups.

In this study, the FE-SEM of WSB and WSB-nZVI samples was investigated to assess the structure of nZVI formed on the biochar (Figure 2). According to FE-SEM results, the nZVI has been formed significantly in the form of tube-like structures on the surface of the WSB, in which particles formed in the form of nanoparticles with a diameter of less than 40 nm are visible. In general, the results obtained from the FE-SEM confirm the nZVI precipitation on the surface WSB.

Table 1. Selected chemical composition of WS, WSB, and WSB-nZVI

Samples	pH	EC (dS m^{-1})	*N(%)	*C(%)	*S(%)	*H(%)	H/C
WS	7.1	0.1	2.63	46.5	0.77	4.68	0.1
WSB	8.3	2.3	2.16	53.6	0.57	2.39	0.04
WSB-nZVI	7.7	1.2	1.9	27.4	0.42	5.7	0.2

*Measured by CHNS analyzer

Efficiency of Cd removal by WSB and WSB-nZVI adsorbents

The results of Cd removal by two adsorbents (WSB and WSB-nZVI) under various defined conditions (Table 2) showed that WSB-nZVI meaningfully decreased higher amount of Cd compared to WSB. Cd removal values ranged from 31.2 to 99.16 % (with an average of 72.59%) in WSB-nZVI samples, while it ranged from 27.16 to 75.25 % (with an average of 39.27%) in WSB

ones. The existence of nZVI on biochar surface in presence of water and oxygen produces a layer of ferrous hydroxide [30], which the nZVI would be visible as a core structure, in which the nZVI is the central part and iron oxides/hydroxides present on its shell surface. The existence of this type of nZVI structure may be effective in pollutants removal due to the creation of specific properties, including the high level of special surface and oxidation/reduction potential.

Table 2. Experimental design based on BBM used in this study

Run order	X1	X2	X3	X4	X5	Cd Removal (%)	Run order	X1	X2	X3	X4	X5	Cd Removal (%)
1	50	5	1.25	40	WSB	37.34	30	50	7	1.25	60	WSB-nZVI	70.40
2	50	5	2	60	WSB	31.06	31	75	5	2	40	WSB	31.97
3	50	5	0.5	20	WSB	47.16	32	50	7	1.25	20	WSB	42.60
4	25	5	2	40	WSB	29.20	33	50	7	0.5	40	WSB	54.96
5	75	5	1.25	20	WSB	35.33	34	75	5	1.25	60	WSB	33.23
6	50	5	1.25	40	WSB	33.06	35	50	7	1.25	20	WSB-nZVI	69.26
7	50	7	2	40	WSB	41.24	36	25	5	1.25	20	WSB	35.60
8	50	5	1.25	40	WSB-nZVI	72.38	37	50	5	2	20	WSB	62.60
9	50	7	0.5	40	WSB-nZVI	95.52	38	25	5	0.5	40	WSB-nZVI	99.16
10	50	5	0.5	60	WSB-nZVI	93.02	39	50	3	1.25	20	WSB	31.08
11	50	7	1.25	60	WSB	48.66	40	75	7	1.25	40	WSB	36.15
12	50	5	1.25	40	WSB-nZVI	36.88	41	50	7	2	40	WSB-nZVI	71.20
13	50	3	0.5	40	WSB-nZVI	43.94	42	50	5	1.25	40	WSB	33.60
14	50	3	1.25	20	WSB-nZVI	82.40	43	50	5	1.25	40	WSB-nZVI	80.40
15	25	3	1.25	40	WSB-nZVI	90.48	44	50	3	2	40	WSB-nZVI	93.04
16	25	5	1.25	20	WSB-nZVI	60.80	45	25	7	1.25	40	WSB-nZVI	88.72
17	75	5	2	40	WSB-nZVI	82.47	46	50	3	0.5	40	WSB	33.20
18	75	5	1.25	20	WSB-nZVI	99.12	47	25	5	0.5	40	WSB	47.52
19	50	5	1.25	40	WSB	34.44	48	25	7	1.25	40	WSB	75.25
20	50	5	2	60	WSB-nZVI	58.22	49	75	7	1.25	40	WSB-nZVI	98.73
21	25	3	1.25	40	WSB	27.16	50	50	5	2	20	WSB-nZVI	31.20
22	75	5	1.25	60	WSB-nZVI	94.45	51	50	5	1.25	40	WSB-nZVI	35.74
23	50	5	0.5	20	WSB-nZVI	90.58	52	50	5	1.25	40	WSB	37.30
24	75	3	1.25	40	WSB	34.41	53	50	3	1.25	60	WSB-nZVI	81.74
25	25	5	1.25	60	WSB-nZVI	54.32	54	75	5	0.5	40	WSB	46.32
26	50	5	0.5	60	WSB	44.20	55	25	5	2	40	WSB-nZVI	64.68
27	50	3	2	40	WSB	29.60	56	75	3	1.25	40	WSB-nZVI	73.69
28	75	5	0.5	40	WSB-nZVI	86.31	57	25	5	1.25	60	WSB	36.72

Table 2. Continued

29	50	3	1.25	60	WSB	29.88	58	50	5	1.25	40	WSB-nZVI	69.44
----	----	---	------	----	-----	-------	----	----	---	------	----	----------	-------

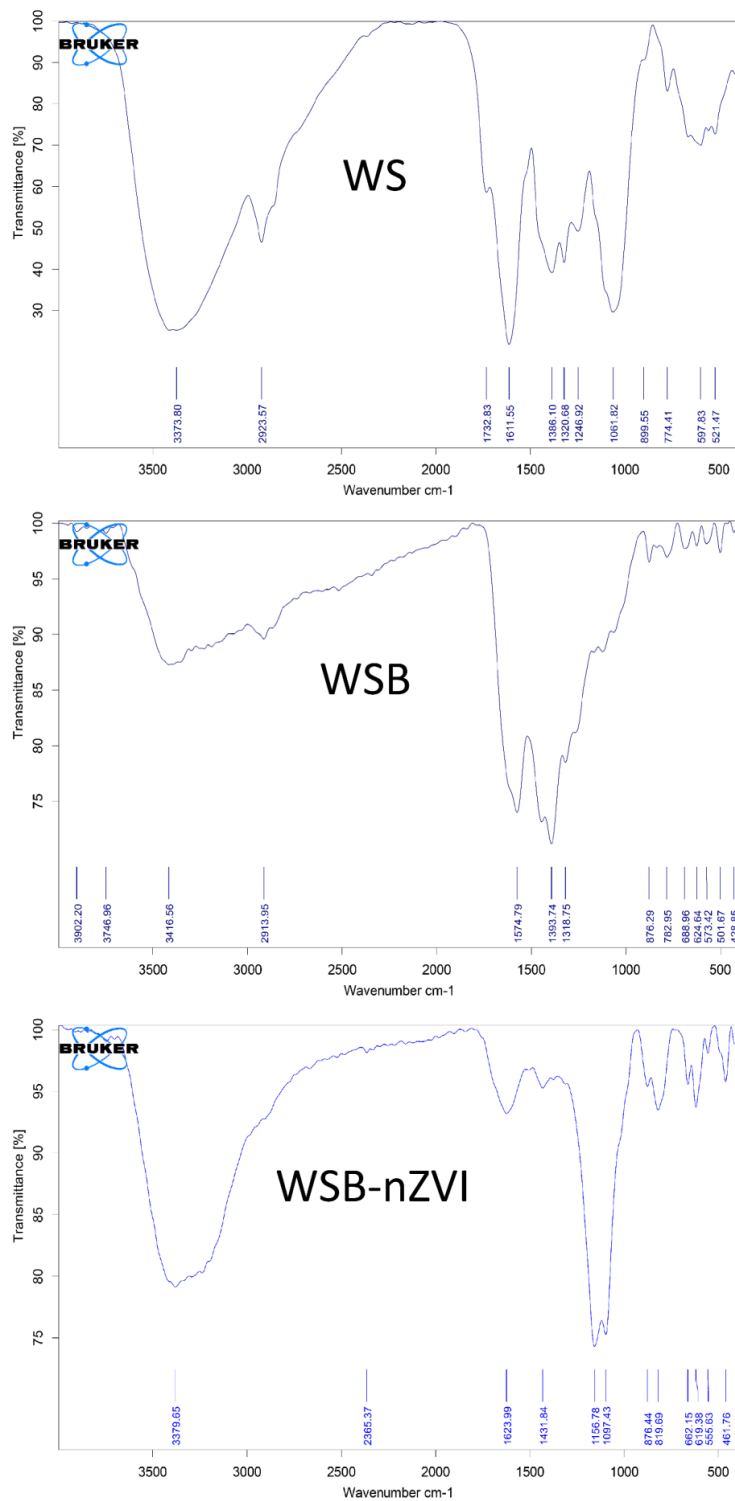


Figure 1. FTIR spectra of WS, WSB, and WSB-nZVI.

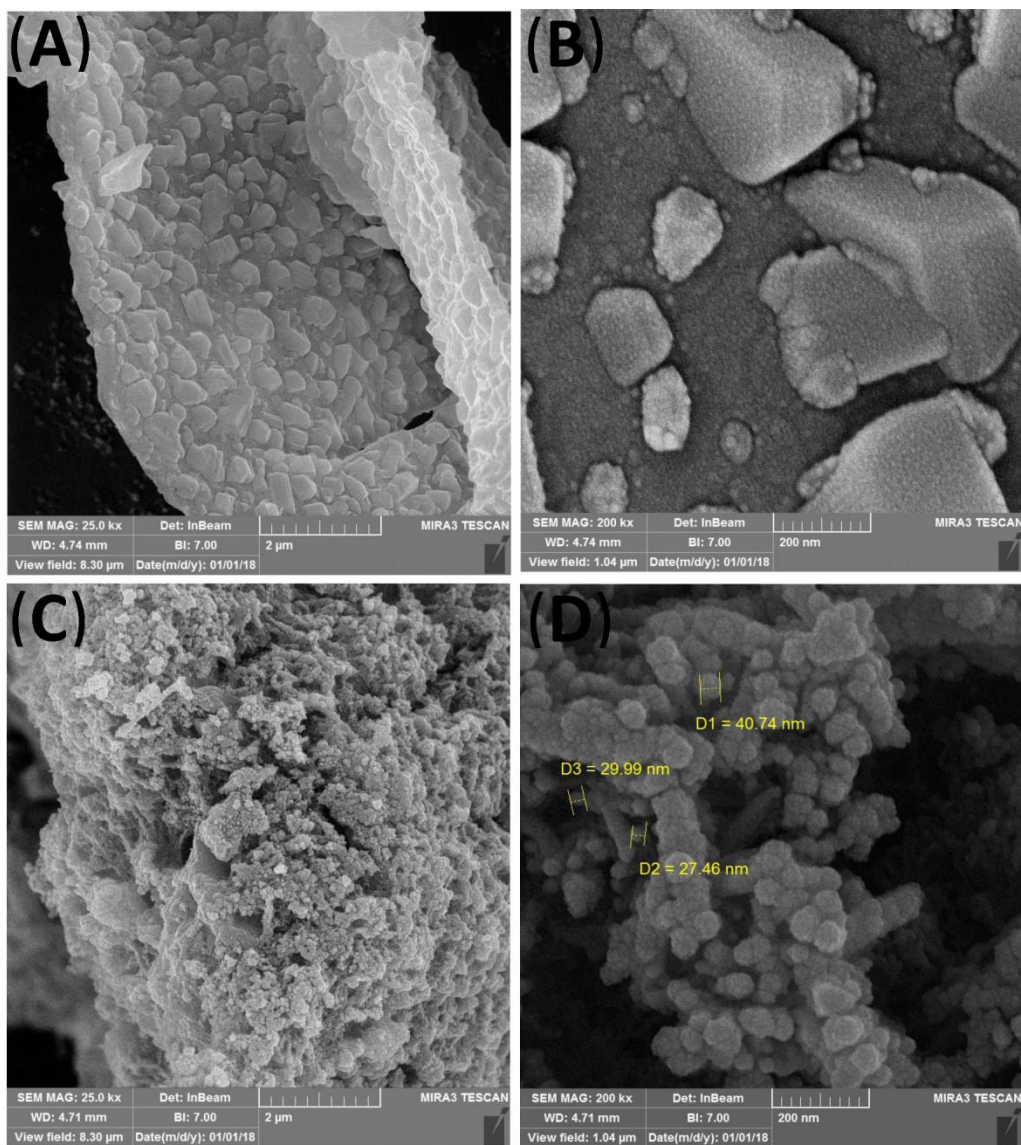


Figure 2. FE-SEM images of WSB [(a): scale 2 μm and (b): scale 200 nm] and WSB-nZVI [(c) scale 2 μm and (d) scale 200 nm].

Studies have shown that elements with a more positive standard potential than iron ($E^0 = -0.41$ V), removal and precipitation processes are considered as important processes for these elements removal [30, 31]. On the other hand, the elements with a standard potential more negative or very close to that of iron, such as Cd ($E^0 = -0.40$ V) are considered as the removal processes as a result of the adsorption or complexation. Therefore, it can be stated that the presence of nZVI on biochar surface has removed Cd from aqueous solutions due to adsorption and complexation processes [30]. Biochars may remove

Cd through several mechanisms such as ion exchange, surface complexation, precipitation and coprecipitation. The addition of nZVI on raw biochar surface, in addition to biochar processes mentioned to eliminate Cd, can help increase Cd removal from aqueous solutions by processes of adsorption and complexation from nZVI. Tan et al [32] stated that impregnation of functional nanoparticles, such as nZVI, onto raw biochar after pyrolysis, (biochar-based composites) could combine the benefits of biochar with the properties of functional nanoparticles. In addition, Sun et al [33] reported

that Cd can eliminate by biochar by three mechanisms, including: 1) ion exchange, 2) surface complexation, and 3) surface precipitation or co-precipitation. So, it is expected that obtained composites (coating of nZVI on biochar surfaces) show both good adsorption (via nZVI part) and surface precipitation or co-precipitation (via WSB part) of Cd on WSB-nZVI. Usman et al [34] assessed sorption process of date palm biochar (prepared at two pyrolysis temperatures of 300 °C and 700 °C) for aqueous Cd removal. They showed that, ion exchange with Ca and Mg, precipitation, or co-precipitation (rather than surface complexation with oxygen-containing functional groups) is the main process for Cd removal by prepared biochar at high pyrolysis temperature. A combination of sorption and precipitation (or co-precipitation) process via nZVI and WSB, respectively, results in the generally high capacity or density per unit surface area for Cd retention. The use of nanomaterials on biochar surface can change heavy metals adsorption through 1) changing on the surface functional groups of biochar and 2) improvement or deterioration on the pore property of biochar [32]. Song et al. [35] and Wang et al. [36] reported that, addition of nanomaterials on the biochar, increased the amount of oxygen-containing functional groups, which higher adsorption of heavy metals occurred [32] by forming surface complexes, cation- π bonding, electrostatic attraction and ion-exchange [35, 36, 37, 38]. Apart from the effect of nZVI, the high effectiveness in reducing the content of those contaminants is probably related with the large specific surface area and the numerous surface functional groups of biochar, which is of fundamental importance in the processes of adsorption of contaminants. In present study, it seems that both the functional groups and nZVI on the surface of biochar could attend for Cd removal in aqueous solutions by process of sorption, precipitation and co-precipitation. The experiments performed under the specified conditions (Table 2) show that the maximum removal of Cd was 99.12%, which is

higher than the values obtained by Doumer et al. [39]. The process of optimizing the design for response surface test has four main stages: (a) the establishment of a suitable test design; (2) proposing a suitable statistical model based on the regression analysis method; (3) verifying the proposed model; and (4) predicting the response variable based on the presented model. The fitting of the results obtained from Cd removal on BBM has created the empirical relationship between non-dependent (un-coded) variables and the efficiency of Cd removal on WSB (Equation 1) and WSB-nZVI (Equation 2) adsorbents, and the corresponding quadratic polynomial equations were obtained as follows:

Equation (1)

$$Y = 115.76 - 1.12X_1 - 6.16X_2 - 8.53X_3 - 0.33X_4 - 0.04X_1X_2 + 0.23X_1X_3 - 0.007X_1X_4 - 6.96X_2X_3 + 0.02X_2X_4 - 0.03X_3X_4 + 0.01X_1^2 + 1.73X_2^2 + 8.46X_3^2 + 0.009X_4^2$$

Equation (2)

$$Y = 83.02 - 1.29X_1 - 2.62X_2 - 1.86X_3 - 0.78X_4 - 0.04X_1X_2 + 0.23X_1X_3 - 0.007X_1X_4 - 6.96X_2X_3 + 0.02X_2X_4 - 0.03X_3X_4 + 0.01X_1^2 + 1.73X_2^2 + 8.46X_3^2 + 0.009X_4^2$$

In addition, relationship between response and variables in coded units has been expressed by the following equation (3):

Equation (3)

$$\begin{aligned}
 Y = & 47.05 + 2.96X_1 + 5.91X_2 - 6.47X_3 - 1.68X_4 \\
 & - 16.67X_5 - 2.44X_1X_2 + 4.32X_1X_3 \\
 & - 3.73X_1X_4 - 2.10X_1X_5 \\
 & - 10.44X_2X_3 + 1.13X_2X_4 \\
 & + 3.54X_2X_5 - 0.50X_3X_4 \\
 & + 2.50X_3X_5 - 4.56X_4X_5 + 9.88X_1^2 \\
 & + 6.94X_2^2 + 4.76X_3^2 + 3.74X_4^2
 \end{aligned}$$

Where: X1, X2, X3, X4, and X5 are Cd concentration, pH, adsorbent dosage, contact time, and kind of adsorbent, respectively.

Analysis of variance (ANOVA) table fitted on quadratic model was used to verify the statistical validity of the model based on significance of the independent variables and their interactions (Table 3) by the student's t-test. The relationship between the mean squares of the model and the error is expressed by the F test. Table 3 shows the regression parameters for the results of predicting the response surface of Cd reduction quadratic model by adsorbents studied in the form of variance analysis. As indicated in Table 3, F probability value achieved in model variable was less than 0.05, indicating the statistical significance of the model fitted on Cd removal data. In other words, this indicates that the predicate quadratic equation is significant and may show many changes at response surface of the regression equation. The closed values of R^2 (0.75) and adjusted R^2 (0.69) show a good correlation between the observed and predicted values as well as high power of the quadratic model in predicting of experimental conditions. Also, the LOF (Lack of fit) value greater than 0.05 indicates the significance of the model fitted to the Cd removal data. Figure 3 shows the relationship between the predicted removal percentage by the statistical model and calculated value. As indicated in the Figure 3, there is an acceptable relationship between the predicted results and the results of the experiment.

Prediction of Cd removal value using RSM

The results obtained in the previous section showed that BBM is a suitable model for predicting the Cd removal influenced by non-dependent variables and their interactions. The geometric display, especially two-dimensional and three-dimensional diagrams, is the best way to improve and explain systems with multiple inputs and outputs. To do so, two-dimensional and three-dimensional graphs were drawn and analyzed to study each variable interaction on Cd removal efficiency. The interaction between initial Cd concentration and pH under predefined conditions (Figure 4) on the Cd removal value showed that in low concentrations of initial Cd, with increasing pH, the Cd removal had a relatively significant increase, although in its high concentrations, in the low pH, the removal was high and it was reduced by increasing the pH to 5, and again increased by increasing the pH to 7. On the other hand, in both low and high pH, the removal percentage has been increased by increasing the value of initial Cd. In low value of pH, the high concentration of hydrogen causes a strong competition between Cd ion and hydrogen to occupy free spaces on adsorbents, which ultimately reduces the Cd from aqueous solutions [16, 40]. Also, reducing the thickness of the dual layer between adsorbent and soluble in aqueous solutions with low pH, may be introduced as a barrier to Cd sorption on adsorbent [41]. In previous studies, it has been shown that, the surface charge of biochar and nZVI would be increased by increasing pH [28]. Therefore, increasing the negative surface charge as a result of pH increasing may be considered as another reason for increasing Cd removal. Increasing the value of Cd removal due to an increase in the initial concentration of Cd may be due to an increase in the Cd gradient transfer capability [42]. Maximum removal of Cd was achieved at pH 7 and initial concentration of 75.

Table 3. Analysis of variance (ANOVA) for quadratic model for Cd removal

Sources of variation	Sum of squares	DF	Mean square	F-value	Probability > F
Model	21522.5	19	1132.76	3.87	< 0.0002
Residual	11101.79	38	206.50		
Lack of fit	7269.57	29	840.92	0.58	0.96
Pure error	3832.21	9	1006.32		
Total	32624.29	57			

$R^2 = 0.75$; Adjusted $R^2 = 0.69$; Predicted $R^2 = 0.57$; CV = 29.95%, DF = Degree of freedom.

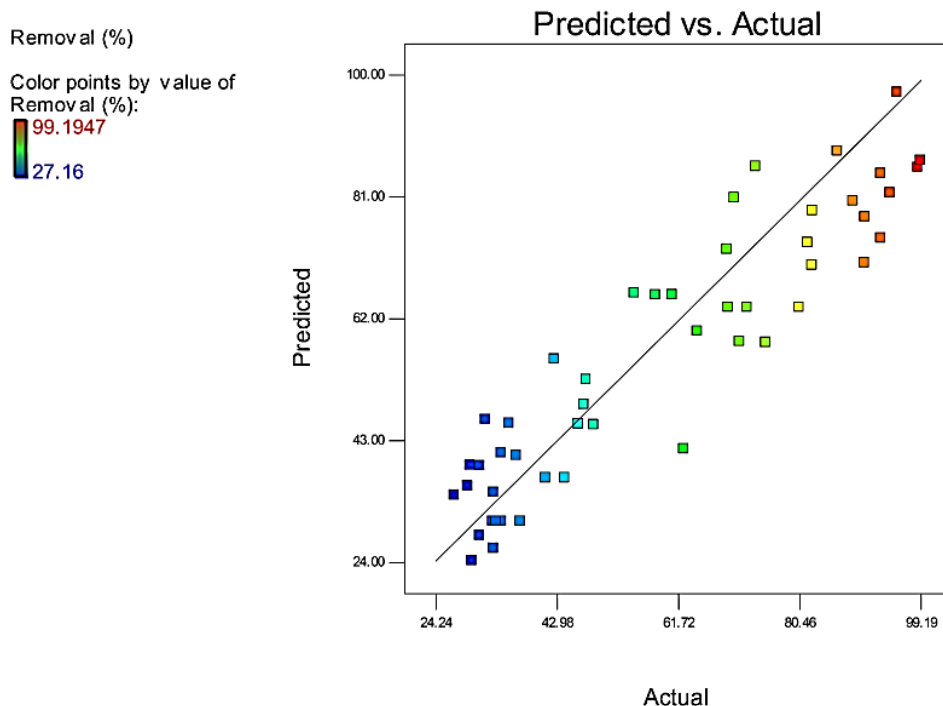


Figure 3. The relationship between the predicted Cd removal percentage by the statistical model and the observed value in the experiments.

The evaluation of interactions between Cd initial concentration and the adsorbent dosage on Cd removal value (Figure 5).

in defined conditions showed that Cd removal value was reduced by increasing the adsorbent dosage, which can be attributed to adsorbents agglomeration at higher dosage [43]. The Cd removal value was high at low concentrations and has been decreased by increasing the concentration to 50 mg L⁻¹ and then it has been increased. Reducing of adsorption from a concentration of 25 to 50 may be explained by the reduction of adsorbent surfaces or, in other words, the saturation of the surfaces available for Cd [44]. On the other hand, increasing of Cd

removal at a concentration of 75 can be due to an increase in the concentration of transition gradient to the adsorbent surface compared to a concentration of 50.

The interactions between initial concentration of Cd and contact time on the efficiency of Cd removal is displayed in Figure 6. As it can be seen, the efficiency of Cd removal has been increased with increasing contact time, which can be explained by the higher accessing of surfaces to Cd ion. Increasing of adsorbent contact with solution at higher concentrations showed an inverse trend, so that the removal rate has shown a decreasing trend by increasing the contact surface, which may be

due to more desorption at the time of contact with the adsorbent with solution.

In the study of the interaction between the solution initial pH and the adsorbent dose on the efficiency of Cd removal value (Figure 7), at low dose of the studied adsorbents, showed the decreasing of removal value with decreasing pH, while the removal trend was reverse at high doses of adsorbent. Maximum adsorption of Cd was found in pH 7 and adsorbent dose of 0.5.

The interaction between contact time and pH on Cd removal value is displayed in Figure 8. The Cd removal value has been increased with increasing the contact time in different ranges of pH. Also, the maximum Cd removal was achieved at maximum pH (7), although the Cd removal change trend dose not relate directly with pH changes, so that the lowest value of Cd adsorption was observed in medium pH of the solution (at the contact time of 20). The Cd removal efficiency influenced by the interaction between contact time and adsorbent dose in the defined conditions (Figure 9) showed that the removal value was increased by increasing contact time and decreasing the adsorbent dose. Decreasing the Cd removal as a result of increasing the adsorbent dose can be attributed to adsorbent agglomeration in the solution, and consequently, to the reduction of the available surface of adsorbents for Cd.

Desirability process

In this research, four different estimates were made according to different types of goals. In the first estimate, all non-dependent variables were considered in defined range and efficiency of Cd removal defined in the maximum. According to this test, 60 solutions were suggested, respectively based on the appropriateness of predictive values, in which the desirability and maximum Cd adsorption values were obtained in the range of 0.24 to 1 and 44 to 99.7%, respectively. In Figure 10(A), the first proposed solution, fitted to the BBM, shows that Cd maximum removal of 99.72% was achieved in the

initial Cd concentration of 70.78 mg L⁻¹, pH of 6.92, adsorbent dose 0.56 g L⁻¹ and contact time of 40.42 min with the desirability of 1. An interesting point in this section is that, among the solutions presented, 28 initial solutions are related to the WSB-nZVI adsorbent, which is the 29th solution of maximum removal of cadmium by 86.35% with the desirability of 0.82 in the initial Cd value of 25 mg L⁻¹, pH 7, adsorbent dose of 0.5 g L⁻¹ and contact time of 20 min for WSB adsorbent. The maximum pH (7) and other non-invariant variables in regulation range as well as the maximum adsorption of Cd were investigated in 2nd test (Figure 10B). The results of this test showed that the maximum adsorption of Cd value of 99.9% was achieved in the initial Cd concentration of 53.44 mg L⁻¹, the adsorption dose of 0.51 g L⁻¹ and the contact time of 57.7 min with the desirability of 1. Maximum adsorption of Cd in this test was based on the solutions proposed related to WSB-nZVI adsorbent. The maximum removal of Cd in the third and fourth tests was studied by considering the adsorbent type of WSB-nZVI and WSB, respectively (other variables was regulated in the range). The maximum value of Cd removal (99.81%) with WSB-nZVI adsorbent was achieved in the initial Cd concentration of 78.15 mg L⁻¹, pH of 6.54, the adsorbent dose of 0.54 g L⁻¹ and contact time of 50.77 min with desirability of 1 (Figure 10C). On the other hand, the maximum removal of Cd (86.35%) with WSB adsorbent was achieved in the initial Cd concentration of 25 mg L⁻¹, pH of 7, adsorbent dose of 0.5 g L⁻¹ and contact time of 20.07 min with desirability of 0.82 (Figure 10D). Rao et al. [45] found that maximum Cd removal of 93.2% by waste agricultural bio-sorbent was obtained at initial Cd concentration 40.15mg L⁻¹, adsorbent dosage 0.5g/50mL solution, pH 5.0, and temperature (35°C), with value of desirability factor 1. According to the results, it can be stated that the maximum adsorption of Cd in both adsorbents was achieved in the highest pH, the lowest dose of the adsorbent, and the maximum contact time. Application of

higher doses of both adsorbents has reduced adsorption. This decrease in adsorption capacity (due to an increase in the amount of adsorbent) can be due to the presence of adsorbents' non-saturated residual adsorption sites during the process, which as a result, with increasing the

amount of adsorbent, a greater amount of it is needed to remove Cd ion. This indicates that the adsorbent changes from the low to high dose acts contrary to the adsorption capacity of adsorbent.

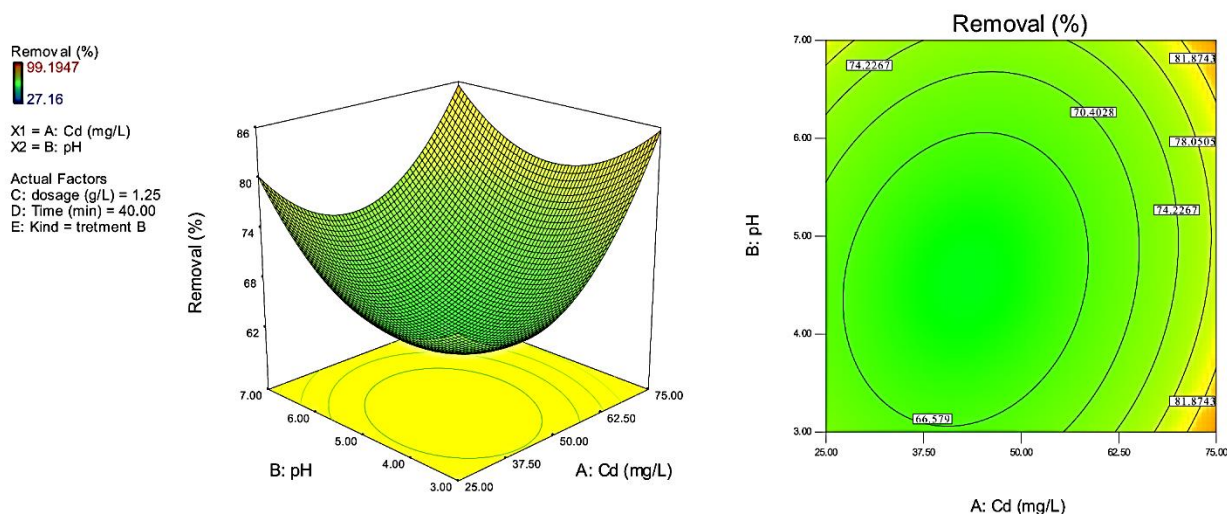


Figure 4. The contour and three-dimensional diagrams of Cd removal efficiency (%) as a function of initial Cd concentration and pH.

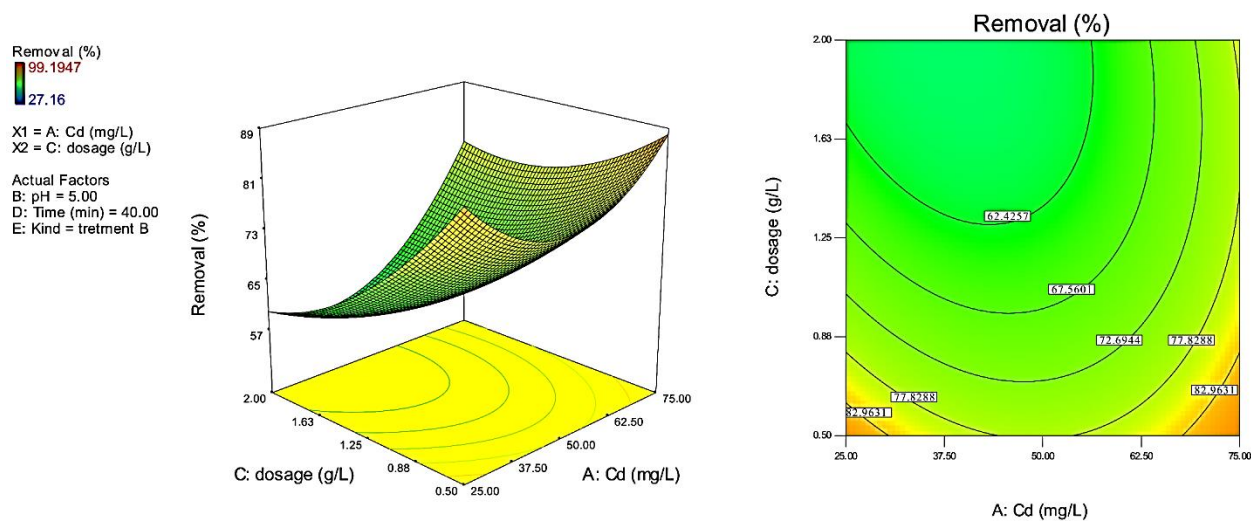


Figure 5. The contour and three-dimensional diagrams of Cd removal efficiency (%) as a function of initial Cd concentration and adsorbent dosage.

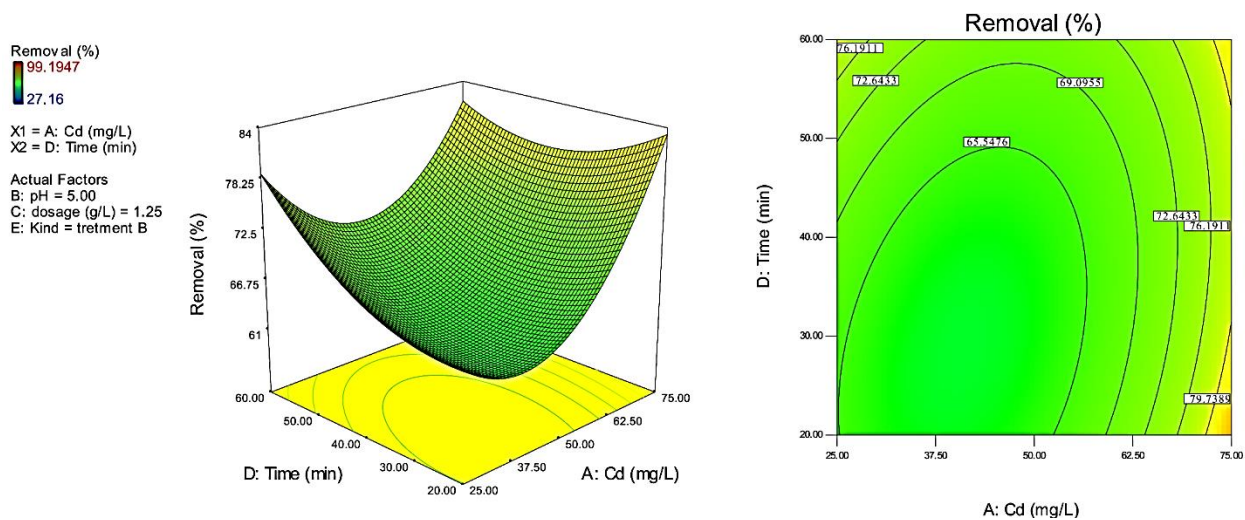


Figure 6. The contour and three-dimensional diagrams of Cd removal efficiency (%) as a function of initial Cd concentration and contact time.

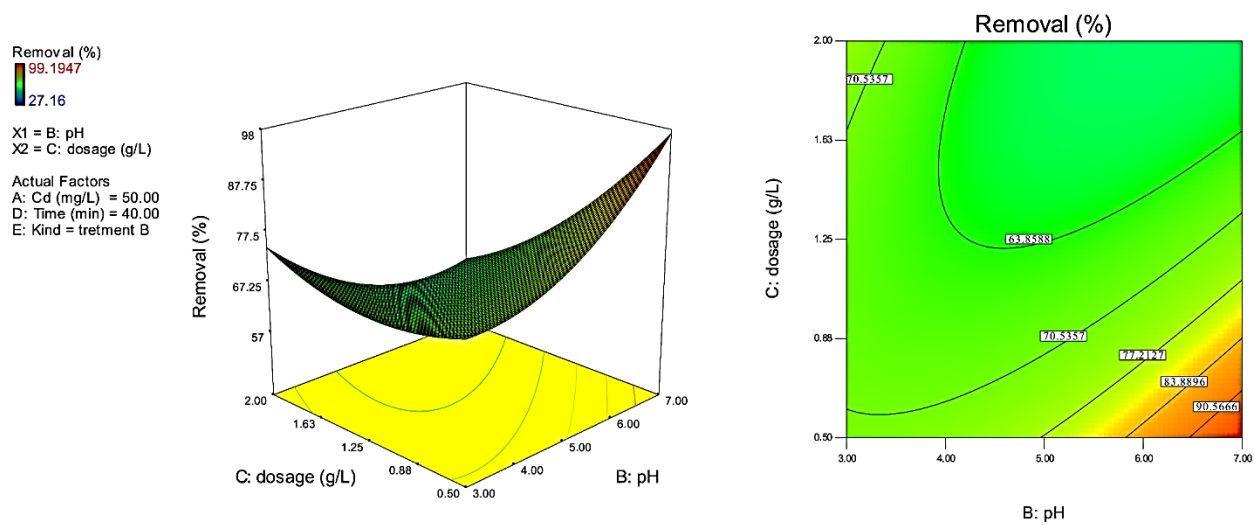


Figure 7. The contour and three-dimensional diagrams of Cd removal efficiency (%) as a function of pH and adsorbent dosage.

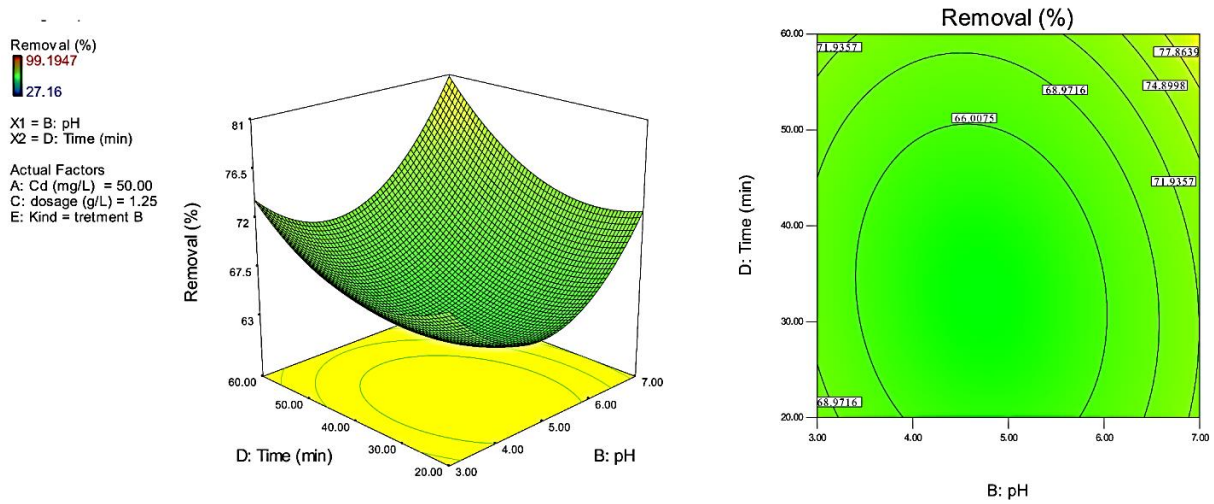


Figure 8. The contour and three-dimensional diagrams of Cd removal efficiency (%) as a function of pH and contact time.

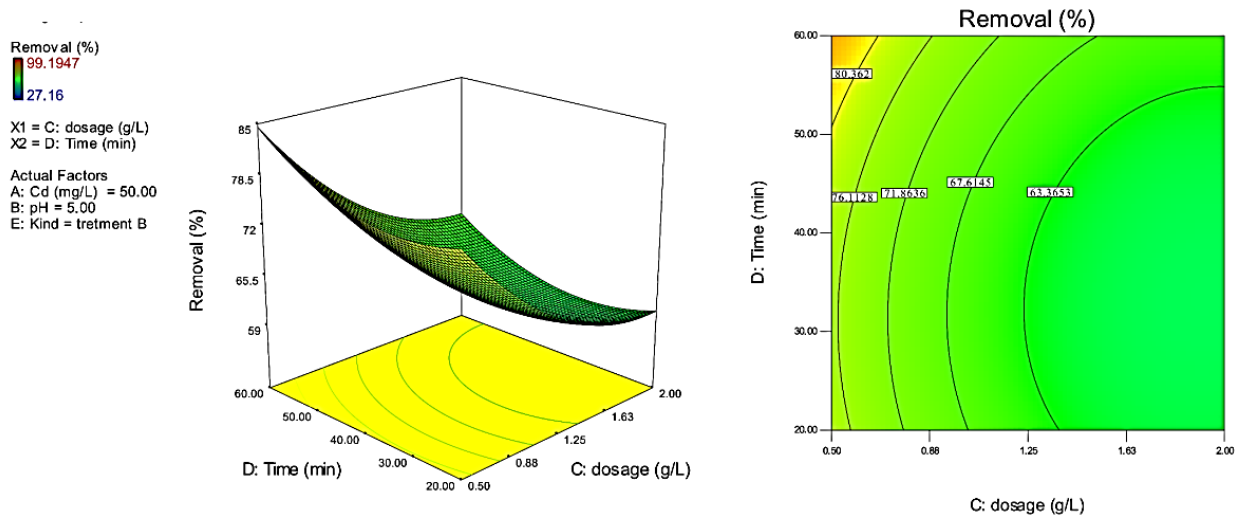


Figure 9. The contour and three-dimensional diagrams of Cd removal efficiency (%) as a function of contact time and adsorbent dosage.

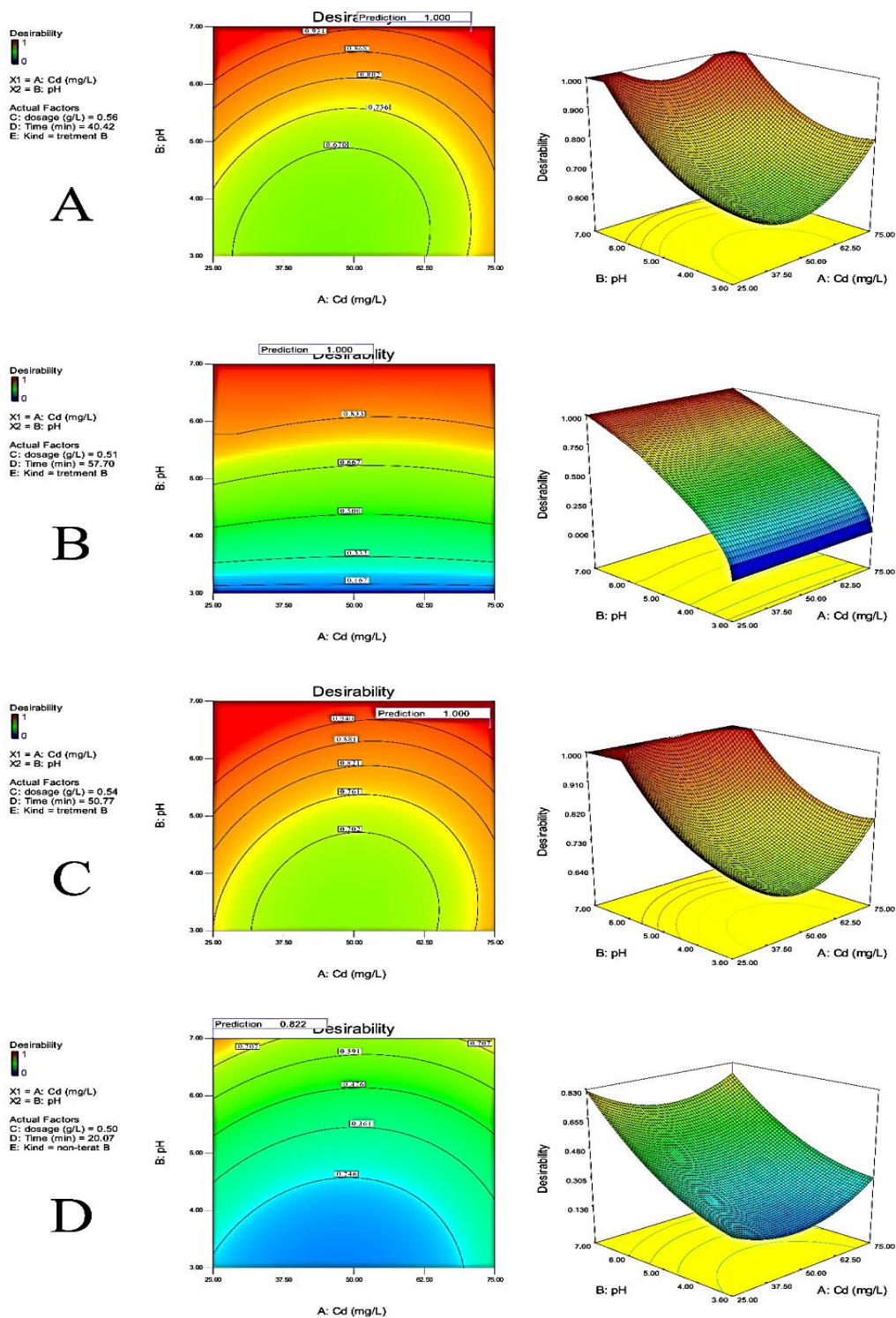


Figure 10. The contour and three-dimensional diagrams of Cd removal efficiency (%) at maximum desirability value and different types of goals (A: all independent variables= within range & response= maximum, B: pH= maximum & other independent variables= within range & response= maximum, C: all independent variables= within range & adsorbent= WSB-nZVI, D: all independent variables= within range & adsorbent= WSB).

CONCLUSIONS

The release of HMs such as Cd in the environment has caused many environmental problems in today's society. In this research, we tried to investigate the efficiency of two adsorbents (WSB and WSB-nZVI) on Cd removal from aqueous solutions under various conditions (initial concentrations of Cd, pH of solution, contact time and adsorbent dose) by BBM. The results showed that WSB-nZVI has a considerable priority to WSB in efficiency of Cd removal in aqueous solutions. The existence of functional groups at the WSB surface, due to the formation of adsorption and precipitation processes, as well as the nZVI formed on the WSB-nZVI sample due to formation of adsorption and complexation processes had increased the ability of Cd removal than WSB raw adsorbent. The maximum efficiency of Cd adsorption predicted by the proposed method was 99.72% with the desirability of 1 at an initial Cd concentration of 70.78 mg L⁻¹, pH of 6.92, adsorbent dose of 0.56 g L⁻¹, and the contact time of 40.42 min. On the other hand, the maximum efficiency of Cd removal from the tests conducted was 99.16% in the initial Cd concentration of 25 mg L⁻¹, pH of 5, the adsorbent dose of 0.5 g L⁻¹, and the contact time of 40 min. In general, the results show a high priority of the WSB-nZVI composition to raw biochar sample (WSB) for Cd removal in various test conditions from aqueous solutions. It seems that the formation of agglomeration is one of the limitations on Cd removal from aqueous solution by the adsorbents mentioned in this study. The application of stabilizing agents is proposed for future studies to prevent agglomeration of this type of adsorbents.

ACKNOWLEDGMENTS

This work has been financially supported by the Institute of Science and High Technology and Environmental

Sciences, Graduate University of Advanced Technology, Kerman, Iran underproject [no. 96.915].

Conflict of interests

The authors declare that there is no conflict of interests.

REFERENCES

1. Awomeso J.A., Taiwo A.M., Gbadebo A.M., Arimoro A.O., 2010. Waste disposal and pollution management in urban areas: a workable remedy for the environment in developing countries. *Am J Environ Sci.* 6(1), 26-32.
2. Wang Q., Yang Z., 2016. Industrial water pollution, water environment treatment, and health risks in China. *Environ Pollut.* 218, 358-365.
3. Nagajyoti P.C., Lee K.D., Sreekanth T.V.M., 2010. Heavy metals, occurrence and toxicity for plants: a review. *Environ Chem Lett.* 8(3), 199-216.
4. Agarwal S., Zaman T., Murat Tuzcu E., Kapadia S.R., 2011. Heavy metals and cardiovascular disease: results from the National Health and Nutrition Examination Survey (NHANES) 1999-2006. *Angiology.* 62(5), 422-429.
5. World Health Organization, 2004. Guidelines for drinking-water quality: recommendations (Vol. 1). World Health Organization.
6. Fu F., Wang Q., 2011. Removal of heavy metal ions from wastewaters: a review. *J Environ Manage.* 92(3), 407-418.
7. Babel S., Kurniawan T. A., 2003. Low-cost adsorbents for heavy metals uptake from contaminated water: a review. *J Hazard Mater.* 97(1-3), 219-243.
8. Sud D., Mahajan G., Kaur M.P., 2008. Agricultural waste material as potential adsorbent for sequestering heavy metal ions from aqueous solutions—A review. *Bioresour Technol.* 99(14), 6017-6027.

9. Lehmann J., Joseph S. (Eds.), 2015. Biochar for environmental management: science, technology and implementation. Routledge.
10. Ahmad M., Lee, S. S., Dou, X., Mohan, D., Sung, J K., Yang, J. E., Ok, Y. S., 2012. Effects of pyrolysi 35 temperature on soybean stover-and peanut shell-derived biochar properties and TCE adsorption in water. *Biore-sour Technol.* 118, 536-544.
11. Yao Y., Gao B., Chen J., Zhang M., Inyang M., Li Y., Yang L., 2013. Engineered carbon (biochar) prepared by direct pyrolysis of Mg-accumulated tomato tissues: characterization and phosphate removal potential. *Bioresour Technol.* 138, 8-13.
12. Zhang M., Gao B., Varnoozfaderani S., Hebard A., Yao Y., Inyang M., 2013. Preparation and characteriza-tion of a novel magnetic biochar for arsenic removal. *Bioresour Technol.* 130, 457-462.
13. Gan C., Liu Y., Tan X., Wang S., Zeng G., Zheng B., Liu W., 2015. Effect of porous zinc–biochar nano-compos- ites on Cr (vi) adsorption from aqueous solution. *RSC Adv.* 5(44), 35107-35115.
14. Zhang M., Gao B., Yao Y., Xue Y., Inyang M., 2012. Synthesis of porous MgO-biochar nanocompo-sites for removal of phosphate and nitrate from aqueous solutions. *Chem Eng J.* 210, 26-32.
15. Tan X., Liu Y., Zeng G., Wang X., Hu X., Gu Y., Yang Z., 2015. Application of biochar for the removal of pollutants from aqueous solutions. *Chemosphere.* 125, 70-85.
16. Boparai H.K., Joseph M., O'Carroll D.M., 2013. Cadmium (Cd²⁺) removal by nanozerovalent iron: sur- face analysis, effects of solution chemistry and surface complexation modeling. *Environ Sci Pollut Res.* 20(9), 6210-6221.
17. Rahmani A. R., Ghaffari H.R., Samadi M.T., 2010. Removal of arsenic (III) from contaminated water by synthetic nano size zerovalent iron. *World Academy of Science, Engineering and Technology.* 62, 1116-1119.
18. Alidokht L., Khataee A.R., Reyhanitabar A., Oustan S., 2011. Reductive removal of Cr (VI) by starch- stabilized Fe⁰ nanoparticles in aqueous solution. *Desal- in.* 270(1-3), 105-110.
19. Esfahani A. R., Firouzi A.F., Sayyad G., Kiasat A., Alidokht L., Khataee A.R., 2014. Pb (II) removal from aqueous solution by polyacrylic acid stabilized zero- valent iron nanoparticles: process optimization using response surface methodology. *Res Chem Intermed.* 40(1), 431-445.
20. Phenrat T., Saleh N., Sirk K., Kim H.J., Tilton R.D., Lowry G.V., 2008. Stabilization of aqueous nanoscale zerovalent iron dispersions by anionic polyelectrolytes: adsorbed anionic polyelectrolyte layer properties and their effect on aggregation and sedimentation. *J Nano- part Res.* 10(5), 795-814.
21. Khuri A.I., Mukhopadhyay S., 2010. Response sur- face methodology. *Wiley Interdisciplinary Reviews: Comput Stat.* 2(2), 128-149.
22. Singh B., Singh B.P., Cowie A.L., 2010. Characteri- sation and evaluation of biochars for their application as a soil amendment. *Soil Res.* 48(7), 516-525.
23. Quan G., Sun W., Yan J., Lan Y., 2014. Nanoscale zero-valent iron supported on biochar: characterization and reactivity for degradation of acid orange 7 from aqueous solution. *Water Air Soil Pollut.* 225(11), 2195- 2199.
24. Box G.E., Behnken D.W., 1960. Some new three level designs for the study of quantitative variables. *Technometrics.* 2(4), 455-475.
25. Ferreira S.C., Bruns R.E., Ferreira H.S., Matos G.D., David J.M., Brandao G.C., Dos Santos W.N.L., 2007. Box-Behnken design: an alternative for the optimization of analytical methods. *Anal Chim Acta.* 597(2), 179- 186.
26. Myers R.H., Montgomery D.C., 2002. Response surface methodology: Process and product improvement with designed experiments.

27. Mukherjee A., Zimmerman A.R., Harris W., 2011. Surface chemistry variations among a series of laboratory-produced biochars. *Geoderma*. 163(3-4), 247-255.
28. Sharma Y.C., 2008. Thermodynamics of removal of cadmium by adsorption on indigenous clay. *Chem Eng J*. 145(1), 64-68.
29. Zhu S., Ho S.H., Huang X., Wang D., Yang F., Wang L., Ma F., 2017. Magnetic Nanoscale Zerovalent Iron Assisted Biochar: Interfacial Chemical Behaviors and Heavy Metals Remediation Performance. *ACS Sustainable Chemistry and Engineering*. 5(11), 9673-9682.
30. Li X.Q., Zhang W.X., 2007. Sequestration of metal cations with zerovalent iron nanoparticles a study with high resolution X-ray photoelectron spectroscopy (HR-XPS). *J Phys Chem*. 111(19), 6939-6946.
31. Huang P., Ye Z., Xie W., Chen Q., Li J., Xu Z., Yao M., 2013. Rapid magnetic removal of aqueous heavy metals and their relevant mechanisms using nanoscale zero valent iron (nZVI) particles. *Water Res*. 47(12), 4050-4058.
32. Tan X.F., Liu Y.G., Gu Y.L., Xu Y., Zeng G.M., Hu X.J., Li J., 2016. Biochar-based nano-composites for the decontamination of wastewater: a review. *Bioresour Technol*. 212, 318-333.
33. Sun J., Lian F., Liu Z., Zhu L., Song Z., 2014. Biochars derived from various crop straws: characterization and Cd (II) removal potential. *Ecotoxicol Environ Saf*. 106, 226-231.
34. Usman A., Sallam A., Zhang M., Vithanage M., Ahmad M., Al-Farraj A., Al-Wabel M., 2016. Sorption process of date palm biochar for aqueous Cd (II) removal: Efficiency and mechanisms. *Water Air Soil Pollut*. 227(12), 449-455.
35. Song Z., Lian F., Yu Z., Zhu L., Xing B., Qiu W., 2014. Synthesis and characterization of a novel MnOx-loaded biochar and its adsorption properties for Cu²⁺ in aqueous solution. *Chem Eng J*. 242, 36-42.
36. Wang H., Gao B., Wang S., Fang J., Xue Y., Yang K., 2015a. Removal of Pb (II), Cu (II), and Cd (II) from aqueous solutions by biochar derived from KMnO₄ treated hickory wood. *Bioresour Technol*. 197, 356-362.
37. Baig S.A., Zhu J., Muhammad N., Sheng T., Xu X., 2014. Effect of synthesis methods on magnetic Kans grass biochar for enhanced As (III, V) adsorption from aqueous solutions. *Biomass Bioenergy*. 71, 299-310.
38. Wang S., Gao B., Zimmerman A.R., Li Y., Ma L., Harris W.G., Migliaccio K.W., 2015b. Removal of arsenic by magnetic biochar prepared from pinewood and natural hematite. *Bioresour Technol*. 175, 391-395.
39. Doumer M.E., Rigol A., Vidal M., Mangrich A.S., 2016. Removal of Cd, Cu, Pb, and Zn from aqueous solutions by biochars. *Environ Sci Pollut Res*. 23(3), 2684-2692.
40. Rao K.S., Mohapatra M., Anand S., Venkateswarlu P., 2010. Review on cadmium removal from aqueous solutions. *Int J EngSci Tech*. 2(7), 81-103.
41. Park D., Lim S.R., Yun Y.S., Park J.M., 2008. Development of a new Cr (VI)-biosorbent from agricultural biowaste. *Bioresour Technol*. 99(18), 8810-8818.
42. Javanbakht V., Zilouei H., Karimi K., 2011. Lead biosorption by different morphologies of fungus *Mucor indicus*. *Int Biodeterior Biodegradation*. 65(2), 294-300.
43. Amini M., Younesi H., Bahramifar N., Lorestani A.A.Z., Ghorbani F., Daneshi A., Sharifzadeh M., 2008. Application of response surface methodology for optimization of lead biosorption in an aqueous solution by *Aspergillus niger*. *J Hazard Mater*. 154(1-3), 694-702.
44. Salmani M.H., Ehrampoush M.H., Sheikhalishahi S., Dehvari M., 2012. Removing copper from contaminated water using activated carbon sorbent by continuous flow. *J Community Health Res*. 1(1), 11-18.
45. Rao K.S., Anand S., Rout K., Venkateswarlu P., 2012. Response surface optimization for removal of cadmium from aqueous solution by waste agricultural biosorbent *Psidium guajava* L. leaf powder. *Clean Soil Air Water*. 40(1), 80-86.

